$\mathbf{D}_{iem}$: Damage Indices for RC columns under three-dimensional seismic action

Haoyu Zhang [1], Chenxi Mao [2]

[1] *Institute of Engineering Mechanics, China Earthquake Administration, Key Laboratory of Earthquake Engineering and Engineering Vibration, Institute of Engineering Mechanics, China Earthquake Administration China Earthquake Administration, concretez@163.com*

[2] *Institute of Engineering Mechanics, China Earthquake Administration, Key Laboratory of Earthquake Engineering and Engineering Vibration, Institute of Engineering Mechanics, China Earthquake Administration China Earthquake Administration,, maochenxi2006@163.com*

Abstract

To improve the damage assessment of RC columns under three-dimensional (3D) seismic action, new damage indices model $\mathbf{D}_{iem}$ are constructed: material damage indices for concrete and steel bar are defined. Based on the 3D fibber-element M-φ analysis program, damage indices of plastic hinge cross-section are calculated by integration of element materials damage indices. It can be used to damage and collapse assessment of various directions of one RC column under 3D seismic action at the same time. Based on the relationship between damage indices and reparability of the materials, rehabilitation evaluation indices for the column are calculated by integration of element materials reparability indices, which can be reference to the structure resilience analysis. $\mathbf{D}_{iem}$ has following features: 1) multi-indices, including collapse indices and rehabilitation indices; 2) direction distinction, a column can have different damage indices in different direction at the same time; 3) applicable to various 3D loading paths, including variation of axial force and random bi-lateral displacement. Damage analysis of 9 tested bi-directional hysteretic RC columns shows that $\mathbf{D}_{iem}$ gives reasonable damage evaluation result.

Keywords: damage indices; three-dimensional seismic action; material damage indices; integration of element materials.

1. Introduction

Damage assessment and rehabilitation evaluation are the key factors to the seismic collapse resistant analysis and resilience evaluation of RC structures. Appropriate seismic damage evaluation model likes a ruler: with the structural seismic response overall taken into account, it can still ensure the assessment objective and precise. Aftershock structure vibration [1] and shaking table test [2] all shows that in actual earthquake, the horizontal displacement path of structure is bi-directional and random, the axial force of the columns are fluctuating; residual lateral displacement of the structures indicating different damage level in various directions. However, the most commonly used damage evaluation models of RC structures, such as story drift angle [3] and Park-Ang damage index model [4], are mainly based on the experimental research under unidirectional horizontal hysteretic load and constant axial force [5]. Research shows that [6-8] bi-directionally loaded columns exhibit more severe damage and more degradation in bending capacity and ultimate displacement compared with the unidirectional loaded one. It is inappropriate for bi-directional seismic structures to apply damage criteria derived from unidirectional seismic analyses directly. Therefore, lots of researches are carried out on bi-directional damage model for RC structures [8-11], which mainly focus on the modification and improvement of Park-Ang damage model, mainly applicable for the components under constant axial force and regular bi-directional hysteretic loading. Whether it is applicable for the structures under random earthquake ground motion is still to be studied. Furthermore, previous studies [6-8] and our experiment analysis [12] both demonstrate that the mechanical properties in orthogonal direction of bi-directional loaded RC columns exhibit obvious correlation, which makes the damage measurement of bi-directional RC columns more difficult than unidirectional ones. More research work needs to be done on bi-directional damage model of RC structures.

This paper focuses on symmetrical reinforcement square cross-section RC frame columns, proposes a new damage model: based on the definition of material (concrete & steel bar) damage models, calculating damage indices of the cross section of plastic hinge by weighted integration. It can be applied to the RC column with axial force variation, random bi-direction displacement path, and the damage differences in various directions also can be considerate.

2. Demage Indices of Integration of Element Materiles (D_{iem})

2.1 Main idea of D_{iem}

Tracing back to the source, structures are constructed by components; components are made up by materials. Structural damage is the macro-scene of the material damage. So a structure damage model based on the material damage definition can be feasible. It can make the damage evaluation based on damage mechanism rather than damage result (hysteretic curves). The connections between materials damage and components damage can be weighted integral calculation, which is accordance with the bending force analysis of cross section of RC components. Different damage evaluation, collapse or rehabilitation, can be achieved by specific integration (fig.1).The key step is the integration of element materials, red circle arrow box in fig.1, so these damage models are together named as **D_{iem}** (**D**amage Indies of **I**ntegration of **E**lement **M**aterials).

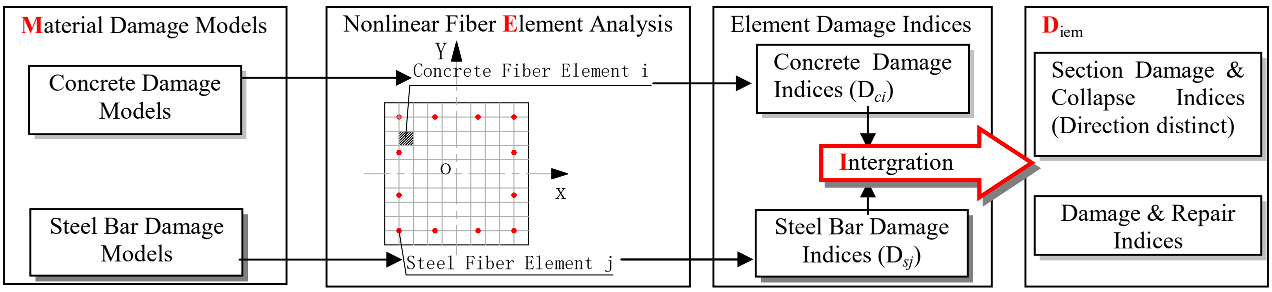

Fig. 1- Main idea of Diem

2.2 Material damage models

2.2.1 Concrete & steel stress-strain model

Material strain-stress relationship definition is the key factors to structural nonlinear analysis. Also material damage definition is the most important step of D_{iem} construction, which is directly depended on the material strain-stress definition. Stress-strain model for confined concrete [13] and path-dependent cyclic stress- strain relationship of reinforcing bar including buckling [14] are selected, implemented by FORTRAN program. Fig.2 shows the hysteretic simulate results of unconfined & confined concrete with f_c=32.3N/mm^2, ε_c=0.0021; f_{cc}/f_c=1.31; Fig.3 shows the simulation of steel bar hysteretic test in REF. [14], which ehxibites good accordance with the experiment.

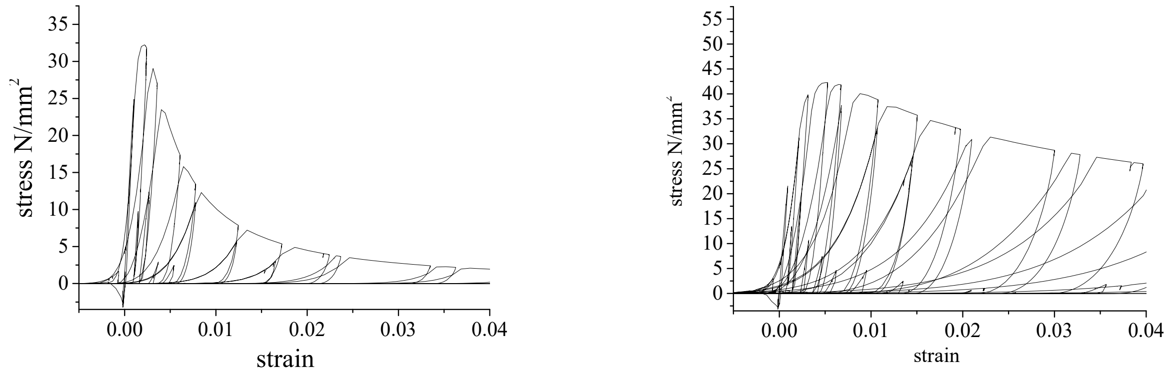

Unconfined concrete　　confined concrete

Fig. 2 - Strain-stress curve of concrete

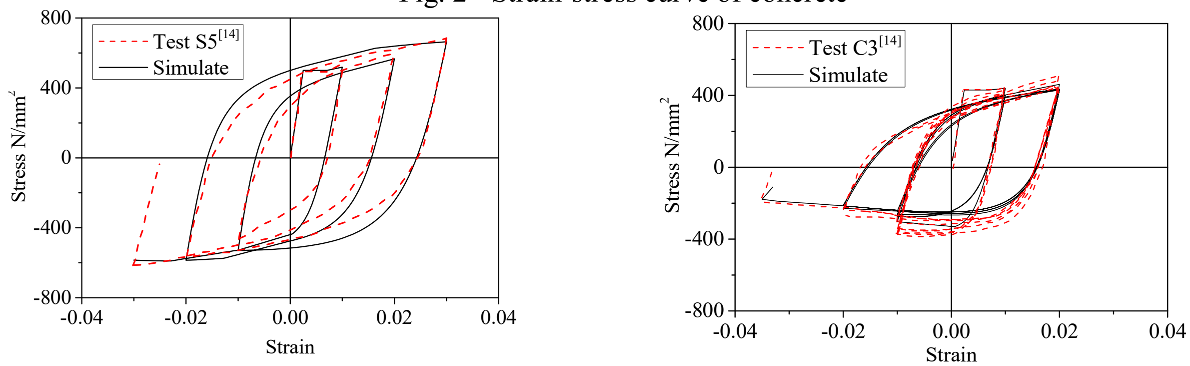

no buckling　　buckling considered

Fig. 3 - Strain-stress curve of steel bar

2.2.2 Concrete damage model

To be accordance with the section damage model D_{sct}, concrete damage model are defined as follows: Compressive failure is the main damage reason of concrete, so the concrete damage index D_{cc} is related to the compressive stress changing, especially the stress drop, represented as the following relationships:

$$D_{cc}=\begin{cases} 0.0 & \varepsilon_c \leqslant \varepsilon_{c0} \\ \dfrac{E_{c0}\varepsilon-\sigma_c}{E_{c0}\varepsilon_{cu}-\sigma_{cu}} & \varepsilon_{c0} < \varepsilon_c \leqslant \varepsilon_{cu} \\ \dfrac{f_{cc}-\sigma_c}{f_{cc}-\sigma_{cu}} & \varepsilon_c > \varepsilon_{cu} \end{cases} \quad (1)$$

Where ε_{c0} is the strain that the concrete begin to be damaged, the point that secant modulus drop to 0.5 times of the tangent modulus of the strain- stress curve is recommended; E_{c0} is the secant modulus of ε_{c0}; σ_{cu} and ε_{cu} are the ultimate stress and ultimate strain, respectively, can be calculated according to Mander[15]. To ensure the applicability to both confined and unconfined concrete, σ_{cu} is recommended limited to $0.85f_{cc}$~$0.5f_{cc}$, f_{cc} is the maximum concrete stress [15].

D_{cc} calculated by Eq. (1) has following characteristics: 1) when D_{cc} is in the range from 0 to 1, it means the concrete stress drop scale from the red dashed line to the real stress in fig.4; when D_{cc}>1, it means the stress drop scale to (f_{cc}-σ_{cu}). Actually, the whole D_{cc} is close to the curve of stress drop scale to (f_{cc}-σ_{cu}), as shown in fig.4. It gives D_{cc} a clear physical meaning – the stress drop scale. Thus in the following damage indices calculation, it makes the damage indices reflect the internal force dropping of the plastic hinge cross section to some extent. Fig.4 also illustrates the relationships between the damage index and the rehabilitation features. It can be references to the post earthquake restoration analysis of the component.

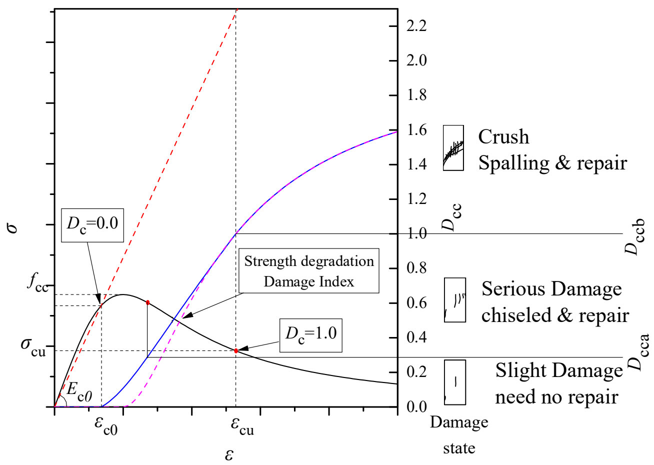

Fig. 4 - Compress damage model of confined (unconfined) concrete

2.2.2 Steel bar damage models

The damage states of the compressed and tentile longitudinal steel bars in plastic hinge are different and relatively independent to some extend. Compressive damage makes the steel bar's streess drop, while tensile damage makes the plastic strain increasing proportionately. So damage models of steel bar are respectively constructed as tensile damage model and compressive damage model.Tensile damage model is given by:

$$D_{st}=\begin{cases} \dfrac{\varepsilon_{s\max}-\varepsilon_{sy}}{\varepsilon_{su}-\varepsilon_{sy}} & \varepsilon_{s\max} \leqslant \varepsilon_{su} \\ 1+5\dfrac{f_{su}-\sigma_s}{f_{su}} & \varepsilon_{s\max} > \varepsilon_{su} \end{cases} \quad (2)$$

Where ε_{smax} is the maximum tensile strain of steel bar, ε_{sy} is yielding strain; ε_{su} and f_{su} are the ultimate strain and ultimate stress of steel bar, respectively, σ_s is the stress of steel bar when the strain is larger than ε_{su}. Fig.5 shows a typical damage index of steel bar, with strain- stress curve attached. It can be reckoned that before the strain reach ε_{su}, damage index is proportional to the plastic strain; once a steel bar's strain larger than ε_{su}, the damage index will increase from 1 rapidly, which can make the weighted integration index reach 1 rapidly.

Compressive damage model is given by:

$$D_{sp} = \begin{cases} 0 & -\varepsilon_{s\min} \leqslant \varepsilon_{sy} \\ \dfrac{\sigma_{st} - \sigma_{sp}}{p_{dc} f_{su}} & -\varepsilon_{s\min} > \varepsilon_{sy} \end{cases} \tag{3}$$

As shown in Fig.6, where ε_{smin} is the minimum strain (compressive, negative) of steel bar; σ_{st} is the tensile stress corresponding to -ε_{smin}, σ_{sp}[14] is the compressive stress corresponding to ε_{smin}. p_{dc} is the stress drop scale factor, can be calculated by Eq. (4).

$$p_{dc} = \frac{f_{cc} - \sigma_{cu}}{f_{cc}} \tag{4}$$

Damage definition above makes the compressive damage model of steel bar has the similar physical meaning with the concrete damage model (Eq.1): compression stress drop scale, which is convenient for the integration damage model to represent the bearing capacity drop scale.

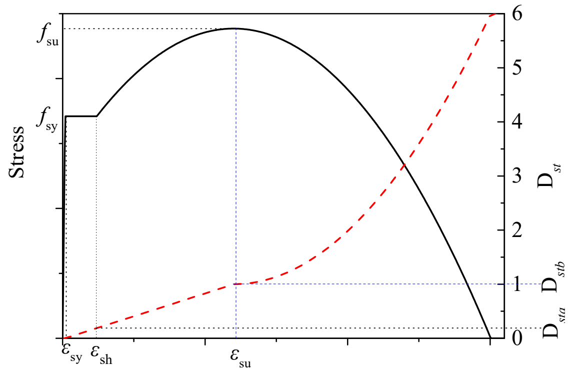

Fig. 5 - tensil damage model of steel bar

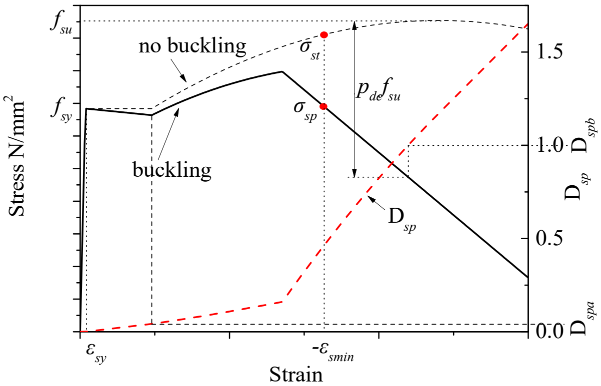

Fig. 6 - compress damage model of steel bar

2.3 Section damage models

Then the section damage indices can be calculated by integration of the element materials' damage indices. Different weighted integral equations can be constructed for different damage evaluations. Most RC columns during the earthquake are compress- bending loaded, so in the cross- section of the plastic hinge, the distance from the fiber element to the centric axis are considered in the integration. In order to distinguish the damage difference in various directions, variety directional centric axes are considered in the calculation. Thus the damage indices are endowed with direction attribute.

2.3.1 Section material bending damage model

As shown in fig.7, for the centric axis, with its included angle to the X axis φ, the corresponding cross-section bending concrete damage index can be calculated by:

$$\mathrm{D}_{c\phi} = \frac{\sum\limits_{x_{\phi i}>0} A_{ci} x_{\phi i} f_{ci} D_{ci}}{\sum\limits_{x_{\phi i}>0} A_{ci} x_{\phi i} f_{ci}} \tag{5}$$

Where $D_{c\varphi}$ is the concrete bending damage index corresponding to direction angle φ; A_{ci} is the area of section concrete element i; $x_{\varphi i}$ is the distance from centro point of concrete element i to the centric axis φy; f_{ci} is the compressive strength of the concrete element i, for the core confined concrete is f_{cc}[13], for the cover concrete is f_c; D_{ci} is the damage index of concrete element i, according to Eq.(1). Only elements with $x_{\varphi i}>0$ are taken into account in Eq. (5).

The section bending steel bar damage index corresponding to the centric axis with its direction angle φ can be calculated by:

$$\mathrm{D}_{s\phi} = \frac{\sum\limits_{ns} A_{sj} x_{\phi j} D_{si}}{\sum\limits_{ns} A_{sj} x_{\phi j}} \tag{6}$$

Where $D_{s\varphi}$ is the section bending steel bar damage index corresponding to the direction angle φ; A_{sj} is the area of steel bar element j; $x_{\varphi j}$ is the distance from centro point of steel bar element j to the centric axis φy; D_{sj} is the damage index of steel bar element j, for compressed steel bar is D_{sp} (Eq.3), for tensile steel bar is D_{st} (Eq.2). All the steel bars are taken into account in Eq. (6).

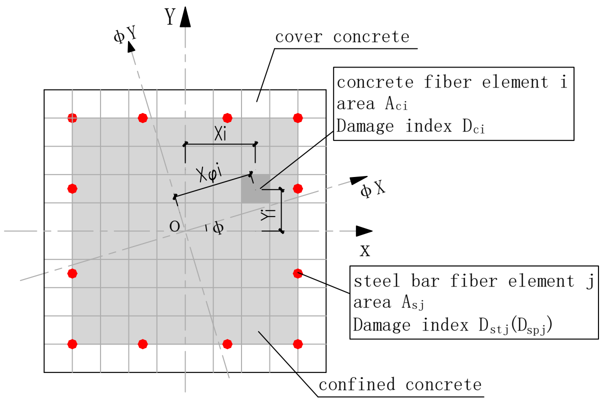

Fig. 7 - Section damage model

Eq. (5) & Eq.(6) are constructed by the following ideas: compression is the mainly stress type of concrete, so only compressive concrete elements are considered in the the section concrete damage index calculation, with its distance to centric axis φy, element area and compressive strength considered in the weighted integration; for steel bar, compressive ones and tensile ones are calculated by the corresponding equations respectively, and with their distance to centric axis φy, element area and yield strength considered in the weighted integration. The calculation above is coordinate with the cross- section moment bending mechanism of RC components.

2.3.2 Section bending damage model

For centric axis with its angle φ, section bending damage index $D_{sct\varphi}$ can be calculated by:

$$\mathrm{D}_{\mathrm{sct}\phi} = \frac{0.5(1-\rho_s)\mathrm{D}_{c\phi}^{\ 2} + \rho_s f_{sy}/f_{cc}\mathrm{D}_{s\phi}^{\ 2}}{0.5(1-\rho_s)\mathrm{D}_{c\phi} + \rho_s f_{sy}/f_{cc}\mathrm{D}_{s\phi}} \tag{7}$$

Where ρ_s is the reinforcement ratio of the longitudinal steel bars; $D_{c\varphi}$ is the section bending concrete damage index (Eq. 5); $D_{s\varphi}$ is the section bending steel bar damage index (Eq. 6).

Eq.(7) are constructed by the following ideas: considering that the concrete damage index and steel bar compression damage index are all measured by stess drop, the section damage index can also be constructed by the force drop. Based on the definition of $D_{c\varphi}$ & $D_{s\varphi}$, we construct the damage index by force weighted intgral, then Eq.(7) can be obtained. Coordination with the Eq. (5), only half of the concrete are considered, so coefficient 0.5 is mutiplied to concrete damge index. Concrete & steel bar damage inices themselves are also considered in the weighted integral, to ensure D_{sct} reach 1 rappidly when significant difference between $D_{c\varphi}$ and $D_{s\varphi}$ appears and either of them exceed 1.

The component is considered as failure when $D_{sct\varphi}$=1. Here the plastic hinge section damage state is as follows: for centric axis direction φ, compressive concrete reaches the ultimate strain ε_{cu}, tensile reinforces steel bars reach the ultimate strain ε_{su}, the stress of compressive reinforces steel bars dropped to p_{dc} on average.

2.3.3 Section damage & repair indices

As shown in fig.4, the concrete repairable states are divided into three stages: (I) basically intact or slight damage, needs no repair; (II) serious damage, needs chiseled and repair; (III) crushed, spalling and needs repair. Stages are distinguished by the concrete damage indices: D_{cca} between state I & II, recommended as 0.3 temporarily; D_{ccb} between state II & III, recommended as 1.0 temporarily. Then by Eq.(8), the area ratios of the concrete need no repair, needs chiseled and repair and spalling and needs repair can be calculated respectively at any time during loading. Also the reinforcement steel bars' repairable states are divided into three stages: (I) basically intact; (II) strength reduction; (III) destroyed. The states are divided by the steel bar damage indices: D_{sta} (D_{spa}) between state I & II, corresponding to the damage index at ε_{sh}; D_{sta} (D_{spa}) between state II & III, recommended as 1.0 temporarily, as shown in fig.5 & fig.6.

$$p_{\text{int}} = \frac{\sum_{D_{ci}<D_{cca}} A_{ci}}{A_c} \qquad p_{ch} = \frac{\sum_{D_{cca}<D_{ci}<D_{ccb}} A_{ci}}{A_c} \qquad p_{\text{sp}} = \frac{\sum_{D_{ccb}<D_{ci}} A_{ci}}{A_c} \tag{8}$$

Where p_{int} is the area ration of basically intact concrete, p_{ch} is the area ration of chisel & repair concrete, p_{sp} is the area ration of spalling & repair concrete.

The case study following will illustrate the representation, physical meaning and advantages of D_{iem}.

3. Programming & Specimen Damage Analysis by D_{iem}

3.1 Programming & experiment

3D nonlinear hysteretic force-displacement simulation based on plastic hinge M-φ fiber element & D_{iem} damage analysis program for cantilever RC column by FORTRAN are compiled. Displacements are calculated with concentrated plastic hinge, with the shear deformation considered [13]. P-Δ effect, random 3-D loading path are all taken into account. Fig.8 shows the program layout.

Ref. [12] presents 9 bi-directional RC frame column hysteretic texts, here are applied in the case study. Fig.9, Table1 and table 2 are the brief information of the experiment. 9 columns are analised respectively, due to limited space, C1 is selected for the case study.

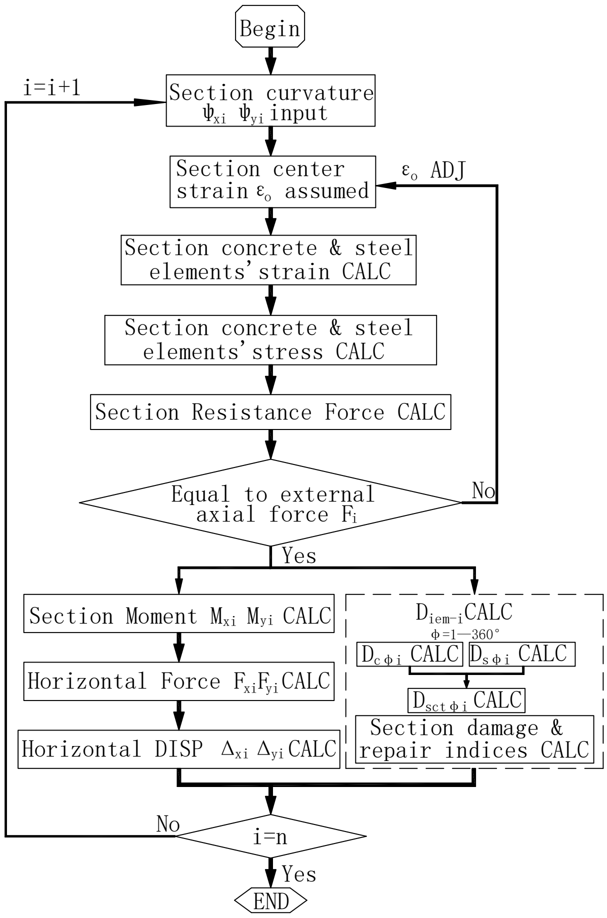

Fig. 8 - Cantilever column analysis program

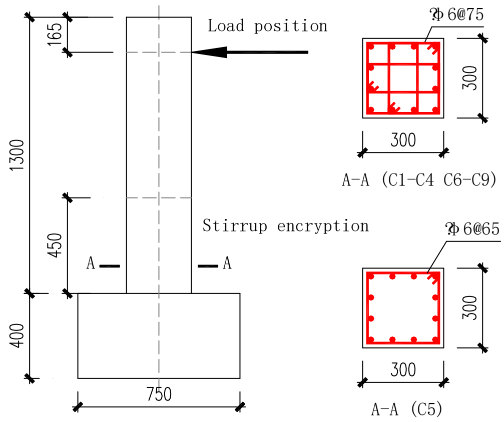

a) specimen dimensions and reinforcement detailing

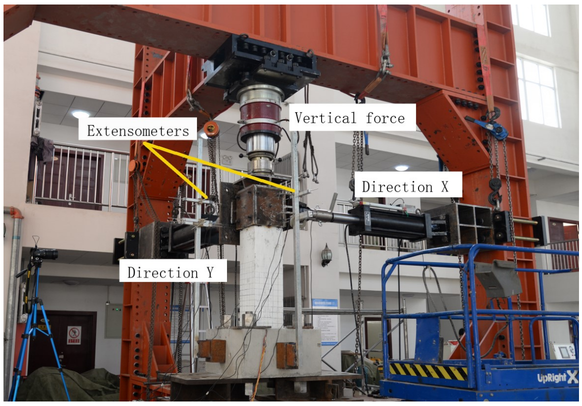

b) test view

Fig. 9 - Experiment sketch[12]

Table1. Specimen specifications & loading path

No.	Axial compression ratio design（actual）	Hoop (Volume stirrup ratio)	Longitudinal steel bars (Reinforcement ratio)	Loading path	
C1	0.60 (0.21)	φ6@75/100(4) (1.16%)	12φ14 (2.05%)	Square	□
C2	0.35 (0.13)	φ6@75/100(4) (1.16%)	12φ14 (2.05%)	Square	□
C3	0.85 (0.30)	φ6@75/100(4) (1.16%)	12φ14 (2.05%)	Square	□
C4	0.60 (0.21)	φ6@75/100(4) (1.16%)	12φ14 (2.05%)	Unidirectional	—
C5	0.60 (0.21)	φ6@65/100(2) (0.67%)	12φ14 (2.05%)	Square	□
C6	0.60 (0.21)	φ6@75/100(4) (1.16%)	4φ12+8φ10 (1.2%)	Square	□
C7	0.60 (0.21)	φ6@50/100(4) (1.70%)	12φ14 (2.05%)	Square	□
C8	0.60 (0.21)	φ6@75/100(4) (1.16%)	12φ14 (2.05%)	Cross	+
C9	0.60 (0.21)	φ6@75/100(4) (1.16%)	12φ14 (2.05%)	Rhombus	◇

Table 2. Mechanical characteristics

Steel bar Diamiter	f_{sy} N/mm^2		f_{su} N/mm^2	Steel bar Diamiter	f_{sy} N/mm^2	f_{su} N/mm^2
6	570		675	12	365	503
10	493		700	14	430	520
Concrete class	f_{cm} (3 specimens each group) N/mm^2			f_{cm}	Standard deviation δ	Standard value f_{ck} N/mm^2
C30	28.4	30.7	32.3	30.5	1.6	27.9

3.2 Damage analysis of C1 by D_{iem}

Fig.10 shows the test X-Y displacement path and X-Y displacement vs. axial load path of C1. The displacement path and the axial load are integrally input into the program, with the key paramenters as follows: f_c=32.3N/mm^2; f_{yv} =600 N/mm^2; f_{cc}/ f_c=1.4; σ_u/ f_{cc}=0.8; f_y=430, f_{su}=520; concentrated plastic hinge with 0.5h (section height) is adopted. The simulate hysteretic curve of horizontal force- displacement at X direction and at Ydirection by the program are shown in fig.11, which are basically accordance with the test results.

It also should be noticed that in fig.11, the blue dash curves show the monotonic pushover simulate result of C1. The peak load of monotonic pushover curve are obviously greater than the one of the bi-directional hysteretic curves. For uni-directional experiment, the difference between peak load of hysteretic skeleton curve and it of monotonic curve is subtle, so the bearing capacity reduced to 85% or 80% of the peak load of the skeleton curve are widely used as the specimen failure criteria. But now the peak load difference bwtween bi-directional hysteretic skeleton curve and monotonic pushover curve may bring uncertainty to the traditional specimen failure criteria.

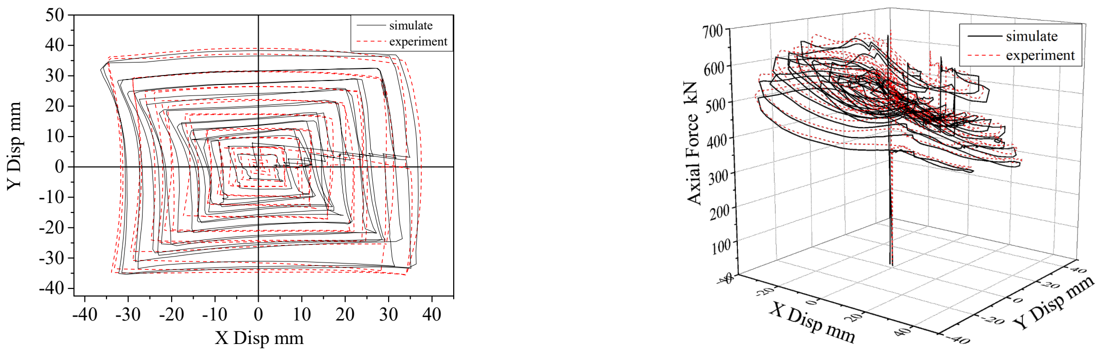

a) X-Y Disp path b) axial force-X Y Disp path

Fig.10- Experimental loading path of C1

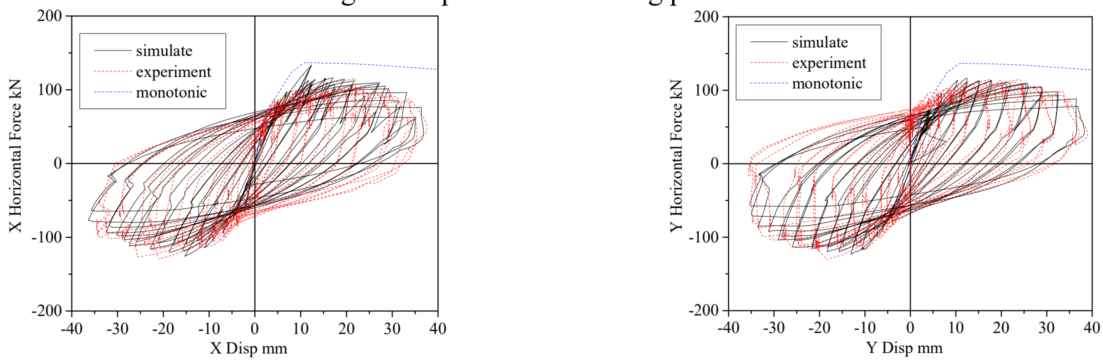

Fig.11 - Shear-drift hysteretic curve of C1

According to Eq.(1) to Eq.(8), D_{iem} histories of C1 experiment are calculated, as shown in fig.12. fig.12 a) shows D_{sct} of bending curvature directions vs. X-Y displacement. The moment that the column became failure can be find exactly. Generally, D_{sct} increasing with the load increasing. Yet some local slight decreases can be found, which is due to the constaintly changing direction of the loading curvatures. Fig.12 b) shows D_{sct} vs. maximum displacement of X direction, the evolution of the damage indices and the failure point can be seen more clearly. According to Eq. (7) and fig.8, at any time of the loading history, φ can be with in 0~2π (0~360°), and the damage index of corresponding direction can be get. Put these indices together into the polar coordinates, **damage circle** we can get. Fig.12 c) shows 4 typical D_{sct} circles of C1, D_{sct} circles with MaxD_{sct}=1 of uniaxial hysteretic load and monotonic load are also presented for contrast. The circles of C1 are generally round, while Y positive is slightly smaller than Y negative. It is because the axial load alternating (fig.10 b), axial load increasing leads to a server damage. In comparison, damage circle of uniaxial hysteretic load is a ellipse, hysteretic directions have the maximum damages; monotonic load damage circle has a obvious deviation to the load direction. Arrange all the damage circles by loading step, we can get the **damage petunia**, as shown in fig.12 d). The damage direction and evolution of the whole loading proccess are illustrated visually by the petunia. Thus the damage circle and the damage petunia give directionality attribute to damage indices. It is helpful to analys the damage (or collapse) direction of RC columns under 3-D seismic action. Fig.12 e) shows the section damage & repair analysis results at D_{sct}=1 of C1 according to 2.3.3. Position and area of different repairability parts are illustrated. According to Eq. (8), area ratio of repairability during the load history are calculated, shown in fig.12f), which is refference to the resilience analysis of the RC column. In fig.12f), the vertical dash marks the area ratio of the concrete at the same loading step of fig.12e). Fig.12 g) shows the damage state of C1 corresponding to the loading step of fig.12 e & f. It appears accordance with the defination that take Dsct=1 as the failure criterion of C1.

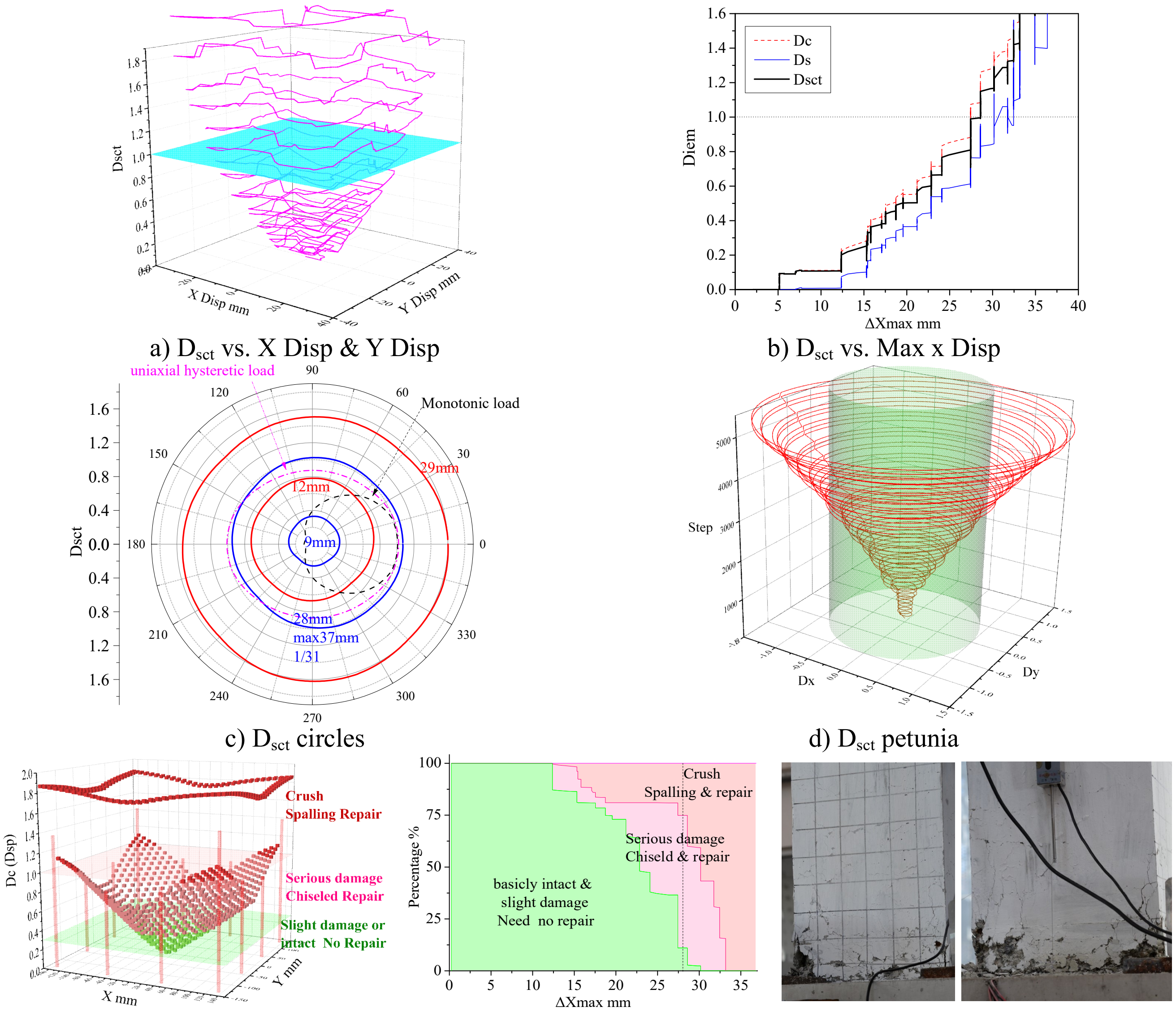

a) D_{sct} vs. X Disp & Y Disp b) D_{sct} vs. Max x Disp

c) D_{sct} circles d) D_{sct} petunia

e) Damage & repair indices f) repair indices vs. loading history g) view of C1 at Dsct=1

Fig. 12- D_{iem} analysis of C1

3.3 Damage comparison of the specimens by D_{sct}

As mentioned in 3.2, to date for bi-directional hysteretic specimens, whether it is reliable to identify the failure displacement by the strength drop percentage of 85% or 80% of its maximum strength is still need to be studied. So in this article, only damage phenomenons of 9 specimens in table.1 are presented for the rationality analysis of D_{sct}. Results are shown in fig.13. On average, it appears fundamentally reasonable to consider Dsct=1 as the failure criterion of RC column. There are slight damage differences among the specimens, which is accordance with the relationship among D_{sct}, D_c & D_s, as mentioned in 2.3.2. So D_{iem} is reliable for 3-D damage analysis of symmetrical reinforcement square section RC column.

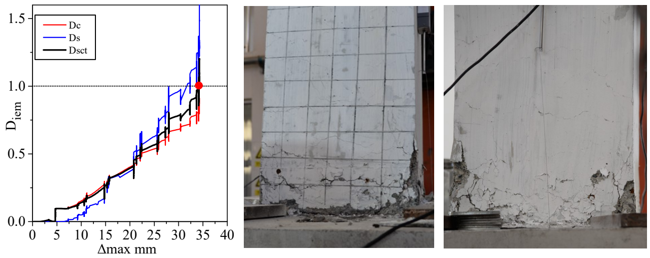

C2 Δ_{max}=34mm 1/33

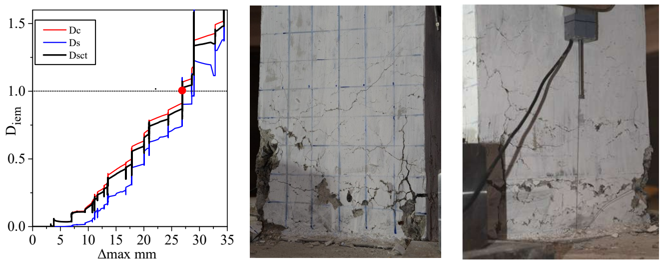

C3 Δ_{max}=26.9mm 1/42

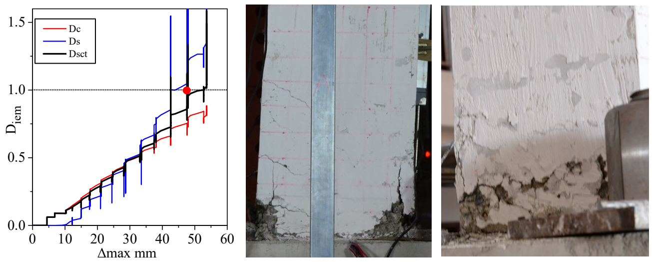

C4 Δ_{max}=47.5mm 1/24 (51.6mm by 85% strength drop percentage of the max. Strength of the skeleton curve)

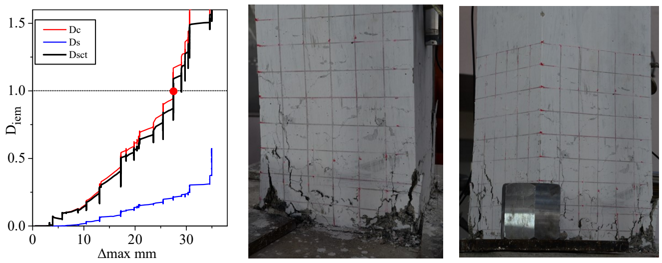

C5 Δ_{max}=27.5mm 1/41

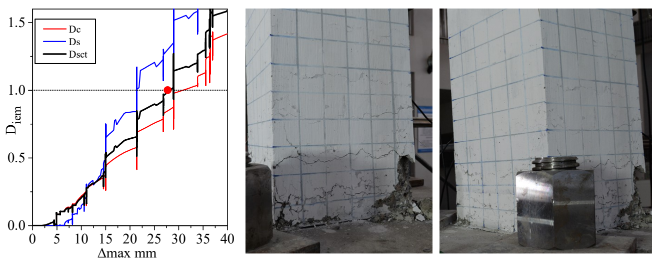

C6 Δ_{max}=26.8mm 1/41

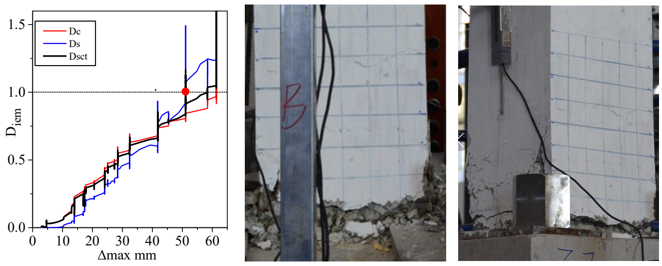

C7 Δ_{max}=51mm 1/22

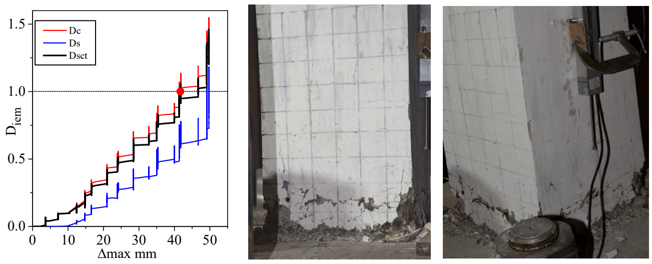

C8 Δ_{max}=42mm 1/27

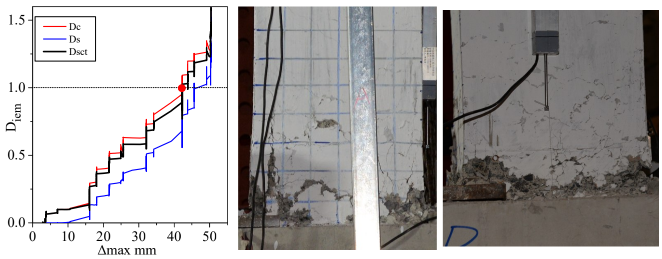

C9 Δ_{max}=42.8mm 1/26

Fig.13- damage comparison of the specimens by D_{sct}

4. Summary and Discussions

According to the studies above, D_{iem} has following features: 1) multi-indices, including material indices, section indices and rehabilitation indices; 2) direction distinction, a column can have different damage indices in various direction; 3) applicable to random 3D loading paths, including variation of axial force and random bi-lateral displacement. Also it is convenient to be applied to the FEM analysis program, without parameters such as the ultimate displacement given in advance.

Meanwhile, D_{iem} are calculated based on the material damage indices definition, which makes it sensitive to the material strain-stress definition and material damage model setup. To ensure the reliability of the damage analysis by D_{iem}, strain-stress parameters' calibration by the material test is necessary, also benchmark model analysis and calibration to unidirectional hysteretic tested specimen are recommended before 3-D seismic damage analysis. In addition, only symmetrical reinforcement square section RC columns are analyzed in this article, the reliability of D_{iem} for un-symmetrical reinforcement rectangular section RC columns is still need to be studied.

5. Acknowledgements

The research presented herein is supported by the funding from IEM (Grant No.2019B02), National Natural Science Foundation of China (Grant Nos. 51108433 and 51678543) and Heilongjiang Province Postdoctoral Science Foundation (Grant No.2016-229). The writers wish to express their sincere gratitude to the sponsors.

6. References

[1] Lemnitzer A, Massone L M, Skolnik D A, et al (2014): Aftershock response of RC buildings in Santiago, Chile, succeeding the magnitude 8.8 Maule earthquake [J]. *Engineering Structures*, **76**:324-338.

[2] Kazuhiko Kasai, Tran-Tuan Nam, Bruce F. Maison (2016): Structural collapse correlative analysis using phenomenological fiber hinge elements to simulate two-directional column deteriorations [J]. *Earthquake Engineering &Structural Dynamics*, **45**:1581–1601.

[3] Federal Emergency Management Agency. FEMA 356 (2000): Prestandard and Commentary for the Seismic Rehabilitation of Buildings[S]. Washington D.C.

[4] Park Y. J, Ang A. H-S (1985): Mechanistic seismic damage model for reinforced concrete [J]. *J. Structural Engineering*, *ASCE*, **4**(111): 722-740.

[5] Lv Xilin, Wang Yayong, Guo Zixiong (2002). The checking calculation of seismic deformation of building structure [J]. *Architecture Science*, **18**(1): 11-15. (In Chinese)

[6] Rodrigues H, Arêde A, Varum H, et al (2013). Experimental evaluation of rectangular reinforced concrete column behavior under biaxial cyclic loading [J]. *Earthquake Engineering & Structural Dynamics*, **42**(2):239–259

[7] Ogimoto H, Kawashima K, Watanabe G, et al (2006): Effect of bilateral excitation on the seismic performance of reinforced concrete bridge columns based on hybrid loading test [J]. *Doboku Gakkai Ronbunshu,* **801**(1):33-50

[8] Qiu F, Li W, Pan P, Qian J (2002): Experimental tests on RC columns under biaxial quasi-static loading[J]. *Engineering Structure,* **24**:419–428.

[9] Rodrigues, Hugo, et al (2013): Damage evolution in reinforced concrete columns subjected to biaxial loading[J]. *Bulletin of Earthquake Engineering*, **11**(5): 1517-1540.

[10] XIA Jan, ZONG Zhouhong (2016): Study on bidirectional seismic damage model of double-skin steel-concrete composite box piers[J]. *Journal of Earthquake Resistant Engineering and Engineering Vibration*, **01**(3): 057-66. (In Chinese)

[11] ZOU Ting (2010): 2D and 3D seismic damage analysis of reinforced concrete frame structures based on OpenSees[D]. *Thesis for the Master Degree in Engineering of Harbin Institute of Technology*. (in Chinese).

[12] ZHANG Haoyu, QU Bowen, MAO Chenxi (2019): Experimental investigation on Seismic Performance of Reinforced Concrete Columns under Biaxial Cyclic Loading[J]. *Journal of Civil Engineering*, **52**(08): 49-61+71. (in Chinese)

[13] G.A. Chang, J.B. Mander (1994): Seismic Energy Based Fatigue Damage Analysis of Bridge Columns: Part 1-Evaluation of Seismic Capacity [R]. *Technical Report NCEER-94-0006.*

[14] Rajesh Prasad Dhakal, Koichi Maekawa (2002): Path-dependent cyclic stress–strain relationship of reinforcing bar including buckling [J]. *Engineering Structures*, **24**:1383-1396.

[15] J.B. Mander, M. J. N. Priestley, R. Park (1988): Theoretical stress-strain model for confined concrete [J]. *J. Structural Engineering*, *ASCE*, **114**(8): 1804-1826.

